ORIGINAL ARTICLE

Methane seep ecosystem functions and services from a recently discovered southern California seep

Benjamin M. Grupe[1], Monika L. Krach[1,*], Alexis L. Pasulka[1,†], Jillian M. Maloney[2,‡], Lisa A. Levin[1] & Christina A. Frieder[1,§]

1 Center for Marine Biodiversity and Conservation, Integrative Oceanography Division, Scripps Institution of Oceanography, University of California San Diego, La Jolla, CA, USA
2 Geosciences Research Division, Scripps Institution of Oceanography, University of California San Diego, La Jolla, CA, USA

Correspondence

Benjamin M. Grupe, University of San Diego, Department of Biology, 5998 Alcala Park, San Diego, CA 92110.
E-mail: bgrupe@ucsd.edu

*Present address: Farallones Marine Sanctuary Association, San Francisco, CA, USA
†Present address: Division of Geological and Planetary Sciences, California Institute of Technology, Pasadena, CA, USA
‡Present address: Department of Geological Sciences, San Diego State University, San Diego, CA, USA
§Present address: Department of Biological Sciences, University of Southern California, Los Angeles, CA, USA

Abstract

The recent discovery of a methane seep with diverse microhabitats and abundant groundfish in the San Diego Trough (1020 m) off the coast of Del Mar, California raised questions about the role of seep ecosystem functions and services in relation to continental margins. We used multicorer and ROV grab samples and an ROV survey to characterize macrofaunal structure, diversity, and trophic patterns in soft sediments and authigenic carbonates; seep microhabitats and taxa observed; and the abundance and spatial patterns of fishery-relevant species. Biogenic microhabitats near the Del Mar Seep included microbially precipitated carbonate boulders, bacterial mats, vesicomyid clam beds, frenulate and ampharetid beds, vestimentiferan tubeworm clumps, and fields of *Bathysiphon filiformis* tubes. Macrofaunal abundance increased and mean faunal δ^{13}C signatures decreased in multicorer samples nearer the seep, suggesting that chemosynthetic production enhanced animal densities outside the seep center. Polychaetes dominated sediments, and ampharetids became especially abundant near microbial mats, while gastropods, hydroids, and sponges dominated carbonate rocks. A wide range of stable isotopic signatures reflected the diversity of microhabitats, and methane-derived carbon was the most prevalent source of nutrition for several taxa, especially those associated with carbonates. Megafaunal species living near the seep included longspine thornyhead (*Sebastolobus altivelis*), Pacific dover sole (*Microstomus pacificus*), and lithodid crabs (*Paralomis verrilli*), which represent targets for demersal fisheries. *Sebastolobus altivelis* was especially abundant (6.5–8.2 fish·100 m^{-2}) and appeared to aggregate near the most active seep microhabitats. The Del Mar Methane Seep, like many others along the world's continental margins, exhibits diverse ecosystem functions and enhances regional diversity. Seeps such as this one may also contribute ecosystem services if they provide habitat for fishery species, export production to support margin food webs, and serve as sinks for methane-derived carbon.

Introduction

The deep sea is popularly described as remote, alien, and disconnected from society, but this vast region covering 64% of the earth's surface contributes many ecosystem functions, as well as ecosystem services benefiting humans (reviewed in Armstrong *et al.* 2012; Thurber *et al.* 2014). In particular, a myriad of human activities acutely affect deep continental margins. These areas host a diversity of habitats that contribute essential fisheries production, mineral and gas resources, and the regulation of gas and climate cycling, carbon sequestration, waste absorption

and ecological systems (Levin & Dayton 2009; Levin & Sibuet 2012).

Continental margin ecosystems have ecological functions including benthic production and trophic transfer, decomposition of organic matter and nutrient remineralization, and carbon sequestration (Levin & Sibuet 2012), and methane seeps may perform many of these functions. Methane seeps play a role in global biogeochemical cycling and elemental transformation of carbon, sulfur, and nitrogen (Hinrichs & Boetius 2002; Dekas *et al.* 2009; Boetius & Wenzhöfer 2013). The anaerobic oxidation of methane (AOM) and associated precipitation of carbonate at cold seeps constitute a major carbon sink in sediments, introducing a mechanism for benthic biogeochemical processes to influence potential greenhouse gas sources (Ritger *et al.* 1987; Reeburgh 2007). The seep biota acts as a methane filter that prevents methane stored in gas hydrates and the deep biosphere from freely entering the hydrosphere and atmosphere; as much as 20–80% of methane carbon may be converted into benthic biomass and carbonate, depending upon fluid flow rates (Boetius & Wenzhöfer 2013).

The microbial biogeochemical processes that depend on reduced compounds (methane, sulfide, and hydrogen) at seeps create chemosynthetic primary production that sustains heterotrophic and symbiont-bearing fauna endemic to cold seeps, as well as background consumers that may aggregate at these productive benthic ecosystems (Levin 2005; Sellanes *et al.* 2008). At a regional scale, seeps are unique ecosystems that add physical, chemical, and biological habitat heterogeneity to continental margins (Cordes *et al.* 2010). High beta diversity at seeps and surrounding regions can enhance the overall species richness, ecosystem function, and biological regulation that can occur on continental margins (Danovaro *et al.* 2008; Levin *et al.* 2010, 2012). Examples of non-endemic seep fauna utilizing the habitat offered by methane seeps include egg-laying sites and nurseries for benthic octopuses and elasmobranchs (Treude *et al.* 2011; Drazen *et al.* 2003), sponge-garden refugia for macro-fauna (Thurber *et al.* 2010), and structural habitat for predatory fish and crabs (Patagonian toothfish, Sellanes *et al.* 2008, 2012; orange roughy, Bowden et al. 2013; sablefish, B. M. Grupe & L. A. Levin, personal observations; lithodid decapods, Niemann *et al.* 2013).

In this investigation, we document a suite of ecosystem functions associated with a methane seep recently discovered in southern California. The Del Mar Methane Seep occurs at the lower boundary of the oxygen minimum zone (OMZ), and with overlying water already hypoxic, benthic fauna and sediments are jointly affected by sharp gradients in oxygen, sulfide, and organic carbon (Treude 2012). Despite knowledge of several methane seeps off southern California, the macrofaunal biology and community structure have previously been examined only at the San Clemente seeps, which occur much deeper than the OMZ at 1800 m [Bernardino & Smith 2010; but see references for other Northeast Pacific seeps at Monterey (Barry *et al.* 1996), Northern California (Levin *et al.* 2003, 2010), and Oregon (Kulm *et al.* 1986; Sahling *et al.* 2002; Levin *et al.* 2010)].

While the deep sea performs a host of ecosystem functions, here we focused specifically on habitat heterogeneity and biodiversity, trophic support for the benthic ecosystem and habitat for demersal megafauna. As the Del Mar Seep was discovered in 2012, another of our objectives was to provide an initial characterization of its habitats and taxa, and we suggest that this site may be representative of other regional seeps within the OMZ. In regards to seep ecosystem functions, we specifically hypothesized that:

1 Biogenic habitats associated with the seep would contribute complex microhabitats and host distinct species assemblages;
2 Macrofaunal density in sediments would increase with proximity to the seep;
3 Species richness would be greater in sediments near the seep periphery than those further away. The OMZ has depressed diversity, as few species are adapted to the stressful physicochemical conditions, but the *in-situ* microbial production and microhabitat diversity at the seep might support more types of species than typical background sediments (*e.g.* Levin *et al.* 2010);
4 Methane-derived carbon (MDC) would be detectable in the benthic food web near sources of seeping fluids, and isotopically light δ^{13}C signatures characteristic of chemosynthesis would be evident in sediment macrofauna but would decline with increased distance from the seep;
5 Densities of demersal megafauna (*Sebastolobus altivelis* and *Microstomus pacificus*) would be relatively high at the methane seep compared with the surrounding seafloor. Moreover, we hypothesized these demersal fish would be more likely to occur specifically with three-dimensionally complex seep microhabitats (carbonate outcrops, rubble, clam beds) than over flat sediments.

Materials and Methods

Study area

This study was conducted at the Del Mar Methane Seep (32°54.25′ N, 117°46.94′ W) at a depth of 1020 m in the northern portion of the San Diego Trough, approximately 50 km west of the Scripps Institution of Oceanography (San Diego, California). This recently discovered seep is situated on a pop-up structure within a series of

strike-slip faults, where a compressional restraining step-over exerts tectonic control to focus upward fluid flux that feeds dense chemosynthetic assemblages (Ryan *et al.* 2012; Maloney 2013). A number of hydrocarbon seeps (methane, tar, petroleum, *etc.*) are known from the Southern California Bight in the Northeast Pacific, with the closest known methane seeps being in the San Clemente Basin (Torres *et al.* 2002, 75 km south) and the Santa Monica Mounds (Paull *et al.* 2008, 140 km north-northwest). The OMZ (<0.5 ml $O_2 \cdot l^{-1}$) above the San Diego Trough extends from approximately 500 to 1000 m, and the oxygen concentrations measured at the Del Mar Methane Seep were about 0.4 ml $O_2 \cdot l^{-1}$ at a depth of 1000 m in both July and December 2012.

Field sampling

Sediment coring, processing, and environmental data
Samples were acquired during three cruises in July 2012 (RV *Melville* leg MV1209), December 2012 [RV *Melville* leg MV1217 with ROV *Triton* (two dives)], and May 2013 [RV *Western Flyer* with MBARI ROV *Doc Ricketts* (dive 472)] (Fig. 1A,B). Three zones around the seep were sampled: the seep center (100% coverage of chemosynthetic bacterial mats and carbonate boulders, Fig. 1E,F,H); the seep periphery (a mix of carbonates, bacterial mats, clams, and non-chemosynthetic sediments, Fig. 1D,G); and sediments further from the seep lacking visual indications of seep activity (*e.g.* no microbial mats or seep endemic fauna), but sometimes containing pieces of clam shells as evidence of past seepage (Fig. 1C). We deployed a multi-corer (tube diameter 9 cm) to collect sediments from sites varying in their proximity to the seep center: we refer to these locations as A_{173} (~173 m from seep center, three multicorer drops), B_{108} (~108 m from seep center, two drops), and C_{32} (~32 m from seep center, two drops) (Fig. 1A, Table 1). Distances are based on GPS coordinates of RV *Melville* corrected to wire position and are accurate within several meters. Additionally, in May 2013 the ROV *Doc Ricketts* collected sediment push cores (diameter 7 cm) from an ampharetid bed (D_{amph}) and adjacent orange microbial mat (E_{mat}) at the edge of the seep center to quantify their communities (Fig. 1A, Table 1; see below for details regarding other ROV sampling).

All sediment cores were sectioned as follows: 0–1 (including sieved water), 1–2, 2–3, 3–5, and 5–10 cm. One core per multicorer drop was sieved on a 300-μm mesh and sorted live to remove macrofauna, protists, and macroscopic microbes for stable isotope analyses, and two or three cores per location or microhabitat were sectioned and preserved in 8% formalin or 70% ethanol for subsequent macrofaunal characterization (Table 1). Microbial and protistan identifications were based solely on morphotype (*e.g. Thioploca* filaments within sheaths, *Beggiatoa* filaments, and *Thiomargarita* cocci occasionally within sheaths), while invertebrate identifications were based on keys, expert taxonomists, and molecular sequencing for those identified to species. Only macro-fauna were quantified for density, diversity, and community structure analyses.

In July and December 2012, conductivity-temperature-depth (CTD) casts were made to obtain hydrographic data (including temperature, salinity, dissolved oxygen, and pH) for each multicorer drop location. Sediments from one core per location were analysed for total organic matter, Chl *a*, phaeopigments, and percent sand and silt-clay. In December, sediment porewater geochemistry was characterized in two multicores at C_{32} and a single push core (diameter 4.5 cm) that ROV *Triton* collected from an orange microbial mat. These were analysed for methane concentration, $\delta^{13}C$ and δ^2H (deuterium) of methane gas, and sulfide concentration (Supporting Information Table S1). Methane concentration was measured using gas chromatography at the California Institute of Technology Environmental Analysis Center (Green-Saxena *et al.* 2012), and sulfide concentration was measured spectrophotometrically using the Cline Assay (Cline 1969). $\delta^{13}C$ and δ^2H of methane gas were measured at the University of California Davis Stable Isotope Facility using a Thermo Scientific GasBench-PreCon trace gas system interfaced to a Delta V Plus Isotope Ratio Mass Spectrometer (Thermo Scientific, Waltham, MA, USA).

ROV dives and carbonate sampling
ROV dives were conducted in December 2012 (Scripps ROV *Triton*) and May 2013 (MBARI ROV *Doc Ricketts*) to explore the Del Mar Methane Seep, collect imagery, conduct a survey of seep microhabitats and megafauna, and collect carbonate rocks, sediment push cores, and megafauna from different microhabitats (Table 1, see ROV video in Supplementary material). As ROV *Triton* did not have a water-tight or partitioned biobox, the communities associated with carbonates collected during its two dives could not be quantified. Six carbonate rocks collected with the ROV *Doc Ricketts* were stored in separated water-tight partitions. Rocks 1–3 (R1–3) came from the seep center, while Rocks 4–6 (R4–6) came from the periphery (Fig. 1B). Upon recovery, macrofauna were picked or allowed to crawl out of rocks, identified and processed for stable isotopes. We calculated density by normalizing counts to the surface area of each rock. Surface area was calculated by covering a rock with a single layer of aluminum foil, which was weighed and compared with the mass of a known surface area. In addition to collection of push cores (described above), a hydraulic suction was used to collect macrofauna from distinct

Table 1. Sampling locations and habitats.

date (dd/mm/yr)	sampling gear	depth (m)	distance (m) to seep, location	habitat sampled	latitude (N)	longitude (W)	stable isotope data	Cores evaluated for macrofauna density
RV *Melville*								
08/07/12	Multicorer	1038[a]	173 m (A)	*Bathysiphon* tubes	32°54.154'	117°46.945'	Yes	3
10/07/12	Multicorer	1038[a]	173 m (A)	*Bathysiphon* tubes	32°54.154'	117°46.945'		3
10/07/12	Multicorer	1038[a]	173 m (A)	*Bathysiphon* tubes	32°54.154'	117°46.945'		3
10/07/12	Multicorer	1030[a]	108 m (B)	*Bathysiphon* tubes, frenulates	32°54.189'	117°46.937'	Yes	3
10/07/12	Multicorer	1030[a]	108 m (B)	*Bathysiphon* tubes, frenulates	32°54.189'	117°46.937'	Yes	3
RV *Melville* with Scripps Inst. of Oceanography ROV *Triton*								
12/12/12	Multicorer	1026[a]	32 m (C)	*Bathysiphon* tubes, polychaete tubes	32°54.274'	117°46.959'	Yes	3
12/12/12	Multicorer	1026[a]	32 m (C)	Polychaete tubes	32°54.264'	117°46.964'	Yes	2
11/12/12	Grab	1020	0 m	Carbonate rocks (3)	[b]		Yes	
11/12/12	Grab	1020	0 m	Vesicomyid clams	[b]		Yes	
13/12/12	Grab	1020	0 m	Carbonate rocks (6)	[b]		Yes	
13/12/12	Grab	1020	0 m	Vesicomyid clams	[b]		Yes	
13/12/12	Push core	1020	0 m	Orange microbial mat	[b]		Yes	
RV *Western Flyer* with MBARI ROV *Doc Ricketts*								
19/05/13	Push core	1020	0 m (D)	Ampharetid bed adjacent to microbial mat	32°54.261'	117°46.944'		2
19/05/13	Suction	1020	0 m	Ampharetid bed adjacent to microbial mat	32°54.263'	117°46.936'	Yes	
19/05/13	Push core	1020	0 m (E)	Orange microbial mat	32°54.261'	117°46.944'		2
19/05/13	Suction	1020	0 m	Orange microbial mat	32°54.261'	117°46.944'	Yes	
19/05/13	Push core	1020	3 m	Muddy tube field	32°54.256'	117°46.946'		1
19/05/13	Suction	1020	3 m	Muddy tube field	32°54.256'	117°46.946'	Yes	
19/05/13	Suction	1020	0 m	White microbial mat	32°54.261'	117°46.944'	Yes	
19/05/13	Suction	1021	11 m	*Bathysiphon* tubes	32°54.242'	117°46.942'	Yes	
19/05/13	Grab R1	1020	0 m	Carbonate covered in white bacterial mat	32°54.259'	117°46.937'	Yes	1 rock
19/05/13	Grab R2	1020	0 m	Carbonate covered in white bacterial mat	32°54.259'	117°46.937'	Yes	1 rock
19/05/13	Grab R3	1020	0 m	Carbonate covered in orange bacterial mat	32°54.261'	117°46.940'	Yes	1 rock
19/05/13	Grab R4	1020	5 m	Carbonate with white, microbial filaments and arborescent foraminifera	32°54.257'	117°46.934'	Yes	1 rock
19/05/13	Grab R5	1020	5 m	Carbonate with white, microbial filaments and arborescent foraminifera	32°54.257'	117°46.934'	Yes	1 rock
19/05/13	Grab R6	1020	6 m	Carbonate with white, microbial filaments and arborescent foraminifera	32°54.257'	117°46.934'	Yes	1 rock
19/05/13	Grab	1020	2 m	Carbonate covered in red bacterial mat	32°54.253'	117°46.935'	Yes	
19/05/13	Grab	1020	3 m	Tubeworms	32°54.259'	117°46.934'	Yes	
19/05/13	Scoop	1020	14 m	Clams	32°54.267'	117°46.934'	Yes	

[a]Depth measurements at multicorer locations were less precise than depth data associated with ROVs and likely were several meters shallower.
[b]GPS location associated with ROV *Triton* was only accurate within ~25 m, so we cannot provide a precise location for these collections; rocks were all collected from the seep center or periphery, orange microbial mat core was taken from the seep center and clams were collected in the seep periphery.
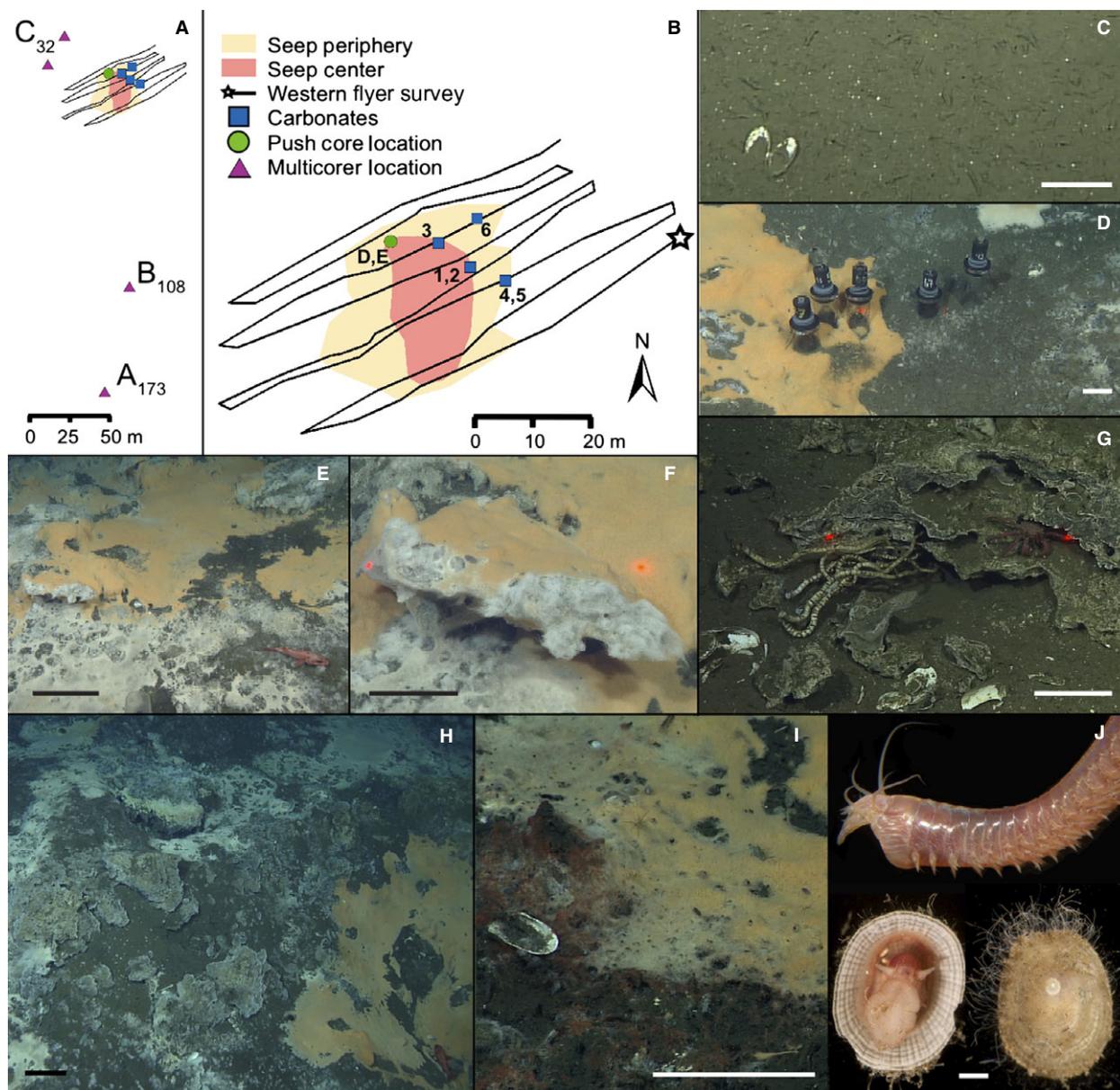
Fig. 1. (A): Multicorer locations (A_{173}, B_{108}, C_{32}) relative to the Del Mar Seep; (B): ROV *Doc Ricketts* survey line and locations of push cores and carbonate rocks (R1–6) collected; (C): sediments away from seep with *Bathysiphon filiformis* tubes; (D): push cores in ampharetid bed (D_{amph}) and orange microbial mat (E_{mat}); (E): seep center with *Sebastolobus altivelis*; (F): carbonate R3, also visible on the left side of (E); (G): small clump of *Lamellibrachia barhami* and a juvenile *Paralomis virrilli* found inside an authigenic carbonate after outer piece of rock was removed; (H): seep center with carbonate boulders and site of possible past hydrate dissociations; (I): diversity of microhabitats at edge of seep center; (J): two of the main consumers of methane-derived carbon are *Nereis* sp. (top) and *Paralepetopsis* sp. (bottom). All scale bars = 10 cm, except (E) and (H) = 30 cm, and (J) is approximately 1 mm. Photo credit: MBARI, except for image J (B. M. Grupe).

microhabitats to sample individuals for stable isotope analysis (Table 1).

ROV video imagery and analysis
During the 19 May 2013 dive with ROV *Doc Ricketts*, to characterize the extent of the methane seep and the abundance of megafauna and their habitat associations, we performed a 45-min visual transect survey of the seep and surrounding seafloor using an Ikegami HDL-40 1920 x 1080i video camera on the ROV. The ROV traversed eight roughly parallel transects of 50 to 80 m each. The total area surveyed was 1437 m²; for analysis this was divided into the seep center (112 m²), seep periphery (317 m²), and off seep (1008 m²) (Fig. 1B).

Video from this survey was used to quantify the density and microhabitat association of the most common megafauna. The ROV *Doc Ricketts* did not pitch or roll, and the camera angle was not altered during the survey. Altitude generally ranged from 1.30 to 1.55 m above the seafloor, corresponding to transect viewing widths of a minimum of 3 m and a maximum of 3.8 m. The total surveyed area for the seep center, seep periphery and off-seep transects was calculated using both the minimum and maximum possible transect widths multiplied by transect length. Latitude and longitude data associated with the ROV were used to map transects and calculate total survey length. Scaling lasers were not used during the survey, so we determined scale by measuring objects of known lengths (*e.g.* aluminum cans, bottles) that appeared at the vertical mid-point of the viewing screen, and were orthogonal with respect to line of sight. Demersal fish and crabs were counted when they passed the screen's mid-point, where lighting was sufficient to accurately identify and measure most megafauna. When an epibenthic species appeared in the frame, we recorded the time, position, location, substrate association (soft sediment, carbonates), and association with biogenic habitat (dead or live clams, bacterial mats, *Bathysiphon filiformis* tubes).

Laboratory and stable isotope analyses

In the laboratory, preserved sediment cores were sieved at 300 μm. All macrofauna were picked using a dissecting microscope and identified to the lowest possible taxonomic resolution (typically genus for gastropods, family for polychaetes, and class or order for other taxa).

For stable isotope analysis ($\delta^{13}C$, $\delta^{15}N$), common representative macrofauna, meiofauna, and macroscopic protists and microbes were sorted shipboard and identified to the lowest feasible taxonomic level. Specimens were left in filtered seawater overnight at 4 °C to clear gut contents, rinsed in milli-Q water, and placed in pre-weighed tin boats using methanol-cleaned forceps. Tissue (0.2–1.4 mg dry weight) was acidified with 12.5–25 μl 2N H_3PO_4 to remove inorganic carbon. To obtain stable isotope signatures of particulate organic carbon, Niskin bottles on a CTD rosette were used to collect water near the surface (~1 m) and from 1000 m. Two liters per sample was filtered through Whatman glass fiber filters, which were scraped, acidified, and analysed in the same manner as tissue samples.

Stable isotope measurements were carried out using a Costech elemental analyzer coupled to a Micromass Isoprime isotope ratio mass spectrometer (EA/IRMS) at Washington State University. Stable isotope ratios ($\delta^{13}C$, $\delta^{15}N$) are expressed in the standard δ (delta) notation and reported in units of per mil (‰) where the element X is represented by:

$$\delta X = \frac{R_{sample}}{(R_{standard} - 1)} \times 1000 \qquad (1)$$

where X is ^{13}C or ^{15}N, and R is the ratio of $\left[\frac{^{13}C}{^{12}C}\right]$ or $\left[\frac{^{15}N}{^{14}N}\right]$. Standards were Pee Dee Belemite for $\delta^{13}C$ and atmospheric nitrogen for $\delta^{15}N$ (Fry 2006).

Statistical analyses

One-way analysis of variance (ANOVA) was used to test whether the fixed factor location had a significant effect on total macrofaunal density, or on the density of the most common taxonomic groups. Data were log-transformed when they did not meet the assumptions of normality or equal variance. Species diversity indices [Shannon index H'_e, Pielou's evenness J', ES_{20}, and ES_{100} (where ES_n is the expected number of species given n individuals)] were calculated for pooled replicates and compared among core locations and carbonate rocks. Rarefaction curves were created to compare taxonomic richness among microhabitats. The influence of locations on community structure was inspected with multivariate analyses of community structure [clustering and nMDS (nonmetric multidimensional scaling) on Bray–Curtis similarity measures] and ANOSIM (Analysis of Similarity) was used to test for differences among locations. Error terms are presented as the standard deviation of the mean unless stated otherwise.

Stable isotope data were inspected with biplots, and one-way ANOVA was used to ask whether microhabitat influenced $\delta^{13}C$ or $\delta^{15}N$ signatures. *Post-hoc* comparisons were carried out with Tukey's HSD (honest significant difference) tests. A single isotope, two-source mixing model (Fry & Sherr 1984) was used to quantify the fraction of MDC making up macrofaunal tissue. The maximum estimated MDC was calculated as:

$$F_m = \frac{(\delta_t - \delta_{POC})}{(\delta_m - \delta_{POC})} \qquad (2)$$

where δ_t, δ_m, and δ_{POC} are the $\delta^{13}C$ signatures of tissue, methane (lighter measurement of −60.4‰) and particulate organic carbon (POC), respectively. The minimum estimated MDC was calculated by substituting δ_{SOB} [$\delta^{13}C$ of sulfur-oxidizing bacteria (SOB)] in place of δ_{POC}, and our heavier $\delta^{13}C$ value of methane for δ_m (−59.4‰) (after Levin & Michener 2002; Thurber *et al.* 2010). Despite the known variability in isotopic methane from seeps (Whiticar 1999; Paull *et al.* 2008), sampling logistics limited us to two measurements of $\delta^{13}C$ of porewater methane (−59.4‰ and −60.4‰, Table S1). We performed

a sensitivity analysis in which δ_m was varied by 10% to examine the effect on MDC calculations.

We used a 2×3 Chi-square test to test the null hypothesis that longspine thornyhead (*Sebastolobus altivelis*) were distributed uniformly among the three habitat zones (expected *versus* observed proportions in the seep center, periphery, and off-seep sediments). Multivariate community analyses were performed in PRIMER 6.1 (PRIMER-E Ltd., Plymouth, UK), rare faction analysis was performed in EstimateS 9.1 (R.K. Colwell, Storrs, CT, USA), and other statistics were performed in JMP 11 (SAS Institute Inc., Cary, NC, USA).

Results

Del Mar Methane Seep microhabitats

Visible features of the Del Mar Seep cover only about 1200 m^2, but encompass a variety of substrate types, microbial mats, symbiont-bearing fauna, and macrofaunal assemblages (see videos S1–S2 in supplementary material). As we expected, taxa were often patchily distributed within particular seep microhabitats (H1). The center of the seep (Fig. 1E) has a heterogeneous topography with carbonate boulders (1–3 m boulder size) and pavement, nearly all covered by extensive orange and white bacterial mats, with signs of possible subsurface methane hydrate (meter-scale pits and craters; Fig. 1H). Red anemones (~3–6 cm diameter) were attached to many carbonates and bacterial mats, which covered most sediments surrounding carbonates. We observed curtains of methane bubbles escaping from the center of orange microbial mats in December 2012 (see video S1) but saw no bubbling in May 2013.

The seep periphery is a halo 10–20 m wide that surrounds the seep center (Fig. 1B). Clam beds (Vesicomyidae: *Calyptogena pacifica*, *Phreagena* 'Calyptogena' *kilmeri*, and *Archivesica* 'Vesicomya' *gigas*) occurred on all sides of the seep periphery, but were less dense to the northeast, which was characterized by carbonate rocks (<10 cm to ~1 m). Vestimentiferan tubeworms (*Escarpia spicata* and *Lamellibrachia barhami*, Fig. 1G) and cladorhizid sponges (*Asbestopluma rickettsii*) were attached to many of these carbonates, often in small aggregations. Substrates in the seep periphery were often covered with fine, white, filamentous bacteria, arborescent foraminifera, and folliculinid ciliates. To the northeast of the seep, sediments contained many inactive carbonates and dead clam shells. By contrast, the seep periphery to the south and west consisted of soft sediments with dense clam beds, extensive shell hash, patchy microbial mats (orange, yellow, red, and white; Fig. 1I) and darker sediments with polychaete tubes (beds of ampharetid polychaetes and the frenulate *Siboglinum veleronis*). No carbonates were observed in the sediments southwest of the seep, but tubes of the large, agglutinated foraminiferan *Bathysiphon filiformis* were observed (Fig. 1C) at every multicorer location, and often were the dominant surface feature.

Sediment macrofaunal assemblage

Proximity to the seep influenced macrofaunal densities, which were greater at sites closer to the center of the seep (Fig. 2; ANOVA, $F_{2,17} = 5.15$, $P = 0.018$). The closest site, C_{32}, had significantly higher macrofaunal density (8888 ± 2435 individuals·m^{-2}) than A_{173}, furthest from the seep (6113 ± 983; Tukey's HSD, $P = 0.017$). The densities of Annelida, Mollusca, and dorvilleid polychaetes were significantly higher at locations closer to the seep (Tukey's HSD, P <0.05, Fig. 2), while several other abundant groups did not vary among locations (Crustacea, Ophiuroidea, and the polychaete families of Paraonidae and Ampharetidae; Fig. 2). Assemblages from these off-seep locations were not significantly distinct (ANOSIM, P > 0.10 for pairwise comparisons among A_{173}, B_{108}, and C_{32}, Supporting Information Fig. S1). Paraonids, bivalves, cirratulids, and ophiuroids contributed nearly half of the similarity observed among these locations (SIMPER results, Supporting Information Table S2).

Both the highest and lowest faunal densities observed came from locations within centimeters of each other in active seep sediments: mean macrofaunal densities were 909 individuals·m^{-2} in the bacterial mat E_{mat}, and 16,240 individuals·m^{-2} in an adjacent ampharetid bed (D_{amph}). Sediments from D_{amph} and the multicores were dominated by Annelida (66% and 78% of all macrofauna, respectively), especially the families Paraonidae (19–24% of individuals at each location), Cirratulidae (4–9%), and Ampharetidae (6–8%) (Fig. 3). Ampharetids made up 65% of the individuals in the push cores in the ampharetid bed, and trochid gastropods (12%) and cuspidarid bivalves (6%) were also common. However, these taxa did not appear in the adjacent microbial mat push cores; the only macrofauna in the mat were juvenile vesicomyid clams and a polynoid and hesionid polychaete.

Carbonate rock assemblage

The density of macrofauna on carbonate rocks, 360 ± 112 individuals·m^{-2}, was over an order of magnitude lower than in sediments. Carbonates were dominated by gastropods (45%, Fig. 3), especially *Provanna laevis* (137.9 ± 86.2 individuals·m^{-2}) and *Pyropelta corymba* (18.2 ± 41.7 individuals·m^{-2}), which typically occurred on the shells of *P. laevis*. Gastropods were significantly more common on Rocks 1–3 from the seep center (255 ± 46 individuals·m^{-2}) than Rocks 4–6 from the seep periphery
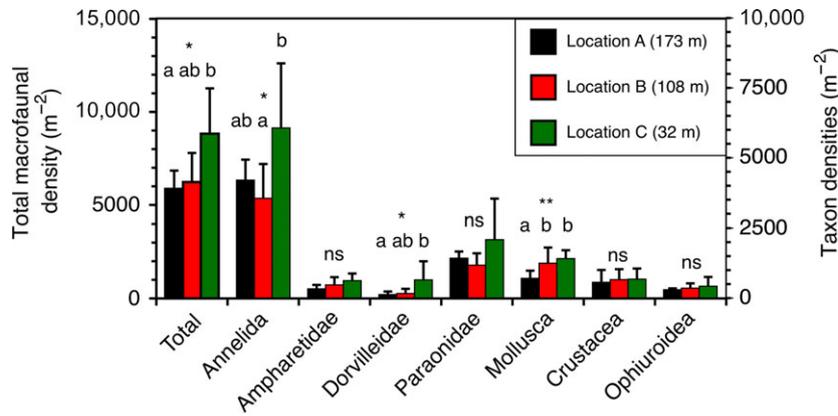
Fig. 2. Macrofaunal densities vary with proximity to the seep. Note that y-axis at left applies to total macrofauna, while y-axis at right applies to individual taxa. Error bars represent SD. Shared letters indicate a lack of significance (Tukey's HSD, *P <0.05, **P < 0.001), while 'ns' indicates non-significant results. Annelida, Dorvilleidae, Paraonidae, and Ophiuroidea were $\log_{(e)}$-transformed to conform to assumptions of normality and equal variances.

(66 ± 25 individuals·m^{-2}, t_4 = 6.15, P = 0.003). Hydroids were common on the carbonates collected from the seep periphery (73 ± 68 individuals·m^{-2}) but absent on those from the seep center. Annelids were much less abundant on carbonates than in sediment cores, but several families represented a higher proportion of total macrofauna on carbonates than they did in sediments away from the seep (Dorvilleidae, 5% *versus* 4%; Polynoidae, 2.7% *versus* 0.6%; Syllidae 4.7% *versus* 0.9%). Communities on carbonates and in sediments were dramatically different (ANOSIM, Global R^2 = 0.603, P < 0.001, Fig. S1), largely due to polychaete groups and bivalves that were abundant in sediments but not carbonates (SIMPER results, Table S2).

Diversity among microhabitats

The rarefaction curves indicate that diversity was very similar for multicores at different locations, with ES$_{100}$ = 25.3–26.3 (Fig. 4, Table 2). Rarified diversity was

much lower in the ampharetid bed (ES$_{100}$ = 11.3) and the orange mat (ES$_{100}$ = 4), a sample from which only seven individuals belonging to four species were recovered. Similarly, Shannon diversity (H′) and Pielou's evenness were highest for multicorer samples far from the seep (2.88–2.97; 0.81–0.86) and lowest for sediments at the seep center (1.35 and 0.54 for D$_{amph}$; indices for E$_{mat}$ were unreliable based on low sample size) (Table 2). For carbonates, rarefied diversity (ES$_{100}$ = 22.7) was slightly lower than for sediments, but much higher than diversity in the ampharetid bed and bacterial mat sediments (Fig. 4). Diversity on carbonates was higher further from the seep center. Compared with the carbonates from the seep center, those from the seep periphery had slightly higher H′ (2.48 *versus* 2.14), J′ (0.79 *versus* 0.69), and ES$_{100}$ (21.2 *versus* 19.3). Sixty types of macrofauna were found across all quantified samples. Of these, 43 occurred in off-seep sediments and 38 were found on seep carbonates, ampharetid beds or microbial mats.
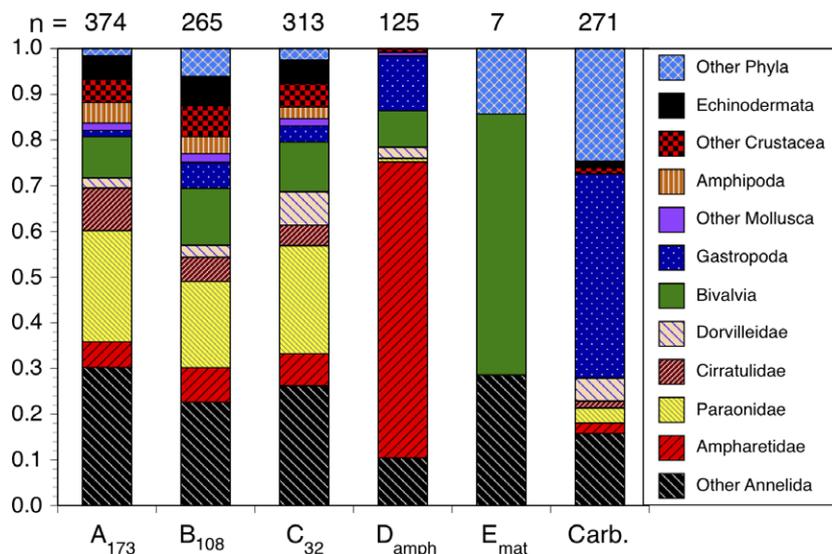

Fig. 3. Faunal composition for sediments and carbonates. Total number of individuals displayed above each bar. Sediments include multicorer locations A$_{173}$, B$_{108}$, and C$_{32}$, and push cores from an ampharetid bed (D$_{amph}$) and an orange micobial mat (E$_{mat}$). Carbonates (C$_{arb.}$) were Rocks 1–6 from the seep center and periphery.

Trophic sources and methane-derived carbon

The stable isotope signatures indicate widespread dependence of macrofauna on both chemosynthetic and photosynthetic primary production (Fig. 5A, Tables 3 and Supporting Information S3). For macrofauna, the range of $\delta^{13}C$ was -15% to -60%, and the range for $\delta^{15}N$ was -9% to $+19\%$. Porewater methane from the Del Mar Seep had an average $\delta^{13}C$ of -59.9% and δD of -184.8% (Table S1), which are indicative of biogenic methanogenesis *via* microbial CO_2 reduction (Whiticar 1999). POC from water samples had a mean ($\pm SD$) $\delta^{13}C$ of $-21 \pm 2.9\%$. Using a two-source mixing model, we estimated that at least 10 seep taxa (five polychaetes, four gastropods, and an encrusting sponge) may depend on MDC indirectly for at least half of their organic carbon (Table 3). The species with the lightest average $\delta^{13}C$ signatures were the patellogastropod limpet *Paralepetopsis* sp. ($\delta^{13}C = -53.5\%$; MDC = 74–84%; Fig. 1J), an oligochaete (-47.5%; 57–69%), a white encrusting sponge (-47.2%; 50–68%), the gastropods *Pyropelta* spp. (-46.4%; 47–66%) and *Provanna laevis* (-41.4%; 29–53%), and the polychaetes *Nereis* sp. (-44.7%; 41–62%; Fig. 1J) and *Dorvillea* sp. (-40.7%; 33–51%). Changing the methane end member by 10% ($\pm 6\%$) caused minimum estimates of MDC to decrease by 1–8%, and maximum MDC to increase by 6–10% (Table S3).

Faunal stable isotope signatures varied significantly by microhabitat ($\delta^{13}C$: ANOVA, $F_{4,406} = 72.3$, $P < 0.0001$; $\delta^{15}N$: $F_{4,245} = 5.09$, $P = 0.0006$). Mean $\delta^{13}C$ was lightest for macrofauna from carbonates ($-35.7 \pm 0.6\%$) and heaviest ($-22.2 \pm 0.5\%$) for those from sediments at A_{173} (Tukey's HSD, $P < 0.05$, Fig. 5B). Macrofauna on carbonates from different zones of the seep exhibited a disparity in isotopic signatures. Macrofauna from Rocks 1–3 at the seep center had significantly lighter $\delta^{13}C$ (-36.2 ± 1.0) and $\delta^{15}N$ ($+3.43 \pm 0.64$) than those from Rocks 4–6 at the periphery (-27.6 ± 1.1, $+9.22 \pm 0.69$, respectively) about 5–10 m from the center of the seep ($\delta^{13}C$: $t_{97} = 5.75$; $\delta^{15}N$: $t_{97} = 6.13$; $P < 0.0001$, Fig. 5B). $\delta^{13}C$ signatures for macrofauna varied among multicorer locations (ANOVA, $F_{2,178} = 3.70$, $P = 0.027$), as A_{173} furthest from the seep had an average $\delta^{13}C$ ($-20.1 \pm 0.8\%$) that was heavier than B_{108} ($-22.3 \pm 0.4\%$; Tukey's HSD, $P = 0.03$), but was not significantly different from C_{32} ($-22.9 \pm 1.1\%$; Tukey's HSD, $P = 0.09$).

Demersal fish and epibenthic invertebrate densities

The dominant megafauna observed during the ROV survey included the longspine thornyhead *Sebastolobus altivelis*, the Pacific Dover sole *Microstomus pacificus*, the lithodid crab *Paralomis verrilli*, and several hagfish

Epta-tretus sp. and zoarcid fish. *Sebastolobus altivelis* was more abundant (6.49–8.22 fish·100 m^{-2}) than *M. pacificus* (0.48–0.60 fish·100 m^{-2}) or *P. verrilli* (0.42–0.54 crabs·100 m^{-2}) (Fig. 6). Although present in all zones around the seep, *S. altivelis* was not distributed randomly and was more likely to occur in the seep center or periphery than away from the seep (Chi-square, $\chi_{test} = 10.26$, $\chi_{crit} = 5.99$, df = 2). Within the seep center and periphery, thornyheads were nearly always next to orange and white microbial mats (*e.g.* Fig. 1E,H), carbonates, clam beds or dead clam shells.

Discussion

Microhabitats and biogenic structure at the Del Mar Methane Seep

The Del Mar Methane Seep interacts with the background continental margin community to create a biomass hotspot with distinct microhabitats and multiple trophic pathways leading to higher trophic levels. The mix of habitats and taxa present reflect the influence of methane, depth, the OMZ, and bathymetry in a highly productive, upwelling margin. Despite the small size of this methane seep, we observed many different microhabitats including sedimented *Bathysiphon* fields, clam beds, orange, white, red, and purple microbial mats, ampharetid beds, and carbonate rocks covered either with microbial mats or with encrusting macrofauna including cladorhizid sponges.

In sediments away from the seep, fields of *Bathysiphon filiformis* and *Siboglinum veleronis* contribute structural heterogeneity and host a relatively diverse suite of soft-sediment macrofauna. Largely typical of the regional OMZ, these are not obligate seep taxa. *Bathysiphon* spp. live in high densities (>100 m^{-2}) in other bathyal environments with high organic flux, such as the Atlantic coast of North America and submarine canyons in New Zealand (Gooday *et al.* 1992; De Leo *et al.* 2010). High surface productivity in the California Current, the location of the Del Mar Seep at the edge of the San Diego Trough, plus seep productivity may combine to create highly organic-rich sediments (15–16% total organic matter, Table S1), leading to high densities of *B. filiformis* tubes. While we did not quantify *Bathysiphon* tubes across all samples, multiple agglutinated tubes were recovered from all multicores, and ROV observations suggest that densities may surpass 200–300 individuals·m^{-2} (*e.g.* Fig. 1C). Frenulate tubeworms, which require sulfide or (in at least one case) methane for their endosymbionts, are common sediment inhabitants in many chemosynthetic settings (*e.g.* Sahling *et al.* 2005; Levin & Mendoza 2007; Hilário & Cunha 2008; Levin *et al.* 2012), but other settings such as the San Diego

Table 2. Diversity indices for macrofauna at all sampling locations at the Del Mar Methane Seep. Rarefied number of species (ES_{20}) is averaged across samples (cores or rocks), and all indices are presented for pooled samples (species richness, ES_{20}, ES_{100}, H', and J').

sampling location	sediments away from seep			ampharetid bed	microbial mat	carbonates		
						seep center	seep periphery	total
	A_{173}	B_{108}	C_{32}	D_{amph}	E_{mat}	Rocks 1–3	Rocks 4–6	Rocks 1–6
replicates averaged								
mean ES_{20}	11.25	11.83	11.61	5.64	2.50[a]	5.78	9.89	8.54
SD	0.68	0.84	1.28	0.39	0.71	3.67	2.16	3.76
SE	0.23	0.34	0.57	0.28	0.5	2.12	1.25	1.53
replicates (cores, rocks)	9	6	5	2	2	3	3	6
replicates pooled								
species	36	32	34	12	4	22	23	31
individuals	374	265	313	125	7	143	129	271
ES_{20} (SD)	11.72 (1.56)	12.23 (1.50)	11.62 (1.62)	5.54 (1.14)	4[a]	8.50 (1.47)	9.90 (1.61)	10.31 (1.78)
ES_{100} (SD)	26.34 (1.70)	26.10 (1.56)	25.28 (1.75)	11.27 (1.12)	4[a]	19.32 (1.73)	21.19 (2.07)	23.04 (2.63)
H'($\log_e$)	2.92	2.97	2.88	1.35	1.15	2.14	2.48	2.59
J'	0.81	0.86	0.82	0.54	0.83	0.69	0.79	0.75

[a]There were not enough individuals present in the microbial mat at Location E to calculate rarefied richness beyond ES_7.

Trough contain organic-rich, reducing sediments that can also support frenulates (Hartman 1961; Hilário *et al.* 2011). While *S. verelonis* is the dominant symbiont-bearing metazoan away from the seep, its density declines near the seep as sulfide levels increase and seep endemic taxa become more abundant, a pattern also observed at the Håkon Mosby mud volcano in the Arctic (Decker *et al.* 2012).

Around the edge of the seep, a patchwork of clam beds, microbial mats, and polychaete tubes was associated with chemosynthetic production and typical seep taxa: bacterial morphotypes resembling *Beggiatoa*, *Thioploca*, and *Thiomargarita*; dorvilleid (*Dorvillea* sp., *Ophryotrocha* sp.), ampharetid, and polynoid (*Bathykurila* n. sp.; S. Katz & G. W. Rouse, personal communication) polychaetes; and at least three species of vesicomyid clams, *Calyptogena pacifica*, *Phreagena kilmeri,* and *Archivesica gigas*. This is a typical assemblage at other Northeast Pacific seeps (Barry *et al.* 1996; Sahling *et al.* 2002; Levin *et al.* 2003). Researchers have hypothesized that evolutionary radiations in these habitats are related to reliance on high sulfide flux and partitioning of microhabitat (Barry *et al.* 1997) and microbial diets (Levin *et al.* 2013). *Calyptogena pacifica* and *P. kilmeri* in particular have been observed at many California and Oregon seeps, where their differing sulfide affinities and growth rates contribute to bulls-eye patterns around bacterial mats as we also observed at the Del Mar Seep (Barry *et al.* 1996; Barry & Kochevar 1998). The nearby Santa Monica mound, however, is dominated by a smaller vesicomyid (*Ectenogena elongata*) that we did not find, perhaps because 1020 m was too deep for this OMZ specialist (Paull *et al.* 2008).

Small patches of dark sediments were common in the seep periphery, and two push cores at D_{amph} confirmed dominance by ampharetids (*Glyphanostomum* sp., 65% of all macrofauna). Our measured macrofaunal density for this habitat was about 16,000 individuals·m^{-2}, which is much lower than the >50,000 macrofauna·m^{-2} described by Thurber *et al.* (2010, 2013) off New Zealand, where tube-building ampharetids engineer sediment habitat *via* bioirrigation and consume aerobic methanotrophic bacteria (Thurber *et al.* 2013). Their occurrence at the Del Mar Seep and Hydrate Ridge, Oregon (L. A. Levin & A. Thurber, personal observations) raises the possibility that macrofauna have similar biogeochemical cycling roles at seeps along the Northeast Pacific continental margin.

Carbonates at the center of the seep contain a faunal assemblage distinct from the surrounding sediments. Fine-scale chemical gradients may also lead to differentiation within carbonate assemblages, as rocks near the seep center were covered with the gastropods *Provanna laevis* and *Pyropelta corymba* and orange or white bacterial mat (Fig. 1F), while rocks several meters away from
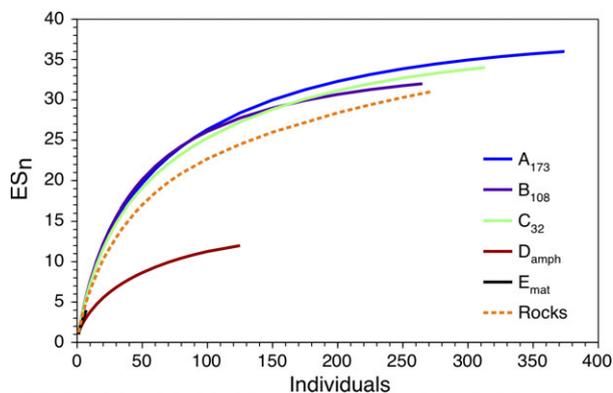
Fig. 4. Influence of microhabitat and proximity to seep on rarefaction of taxonomic richness. Macrofauna from multicores (A_{173}, B_{108}, and C_{32}) and push cores in the ampharetid bed (D_{amph}) and microbial mat (E_{mat}) are pooled by location, and all carbonate macrofauna are included in Rocks. Note that E_{mat} is particularly short as we found only seven individuals in two cores.

the center of the seep had a finer covering of bacterial filaments, arborescent foraminifera, hydroids, and different species of sponges including the newly described cladorhizid *Asbestopluma rickettsii* (Lundsten *et al.* 2014). The dominance of gastropods on seep carbonate is not surprising as they are commonly associated with carbonates in active seep settings on which they graze bacteria (Ritt *et al.* 2010; Levin *et al.* 2012; B. M. Grupe & L. A. Levin, unpublished data). An Elachisinidae gastropod (*Laeviphitus verduini*) and a Mytilidae bivalve made up 75–90% of the macrofauna on carbonates inspected by Ritt *et al.* (2010) at a Mediterranean seep, but mytilids do not appear at the Del Mar Seep. The vestimentiferans *Lamellibrachia barhami* and *Escarpia spicata* are very common at the San Clemente seeps (Bernardino & Smith 2010), but only occurred in small clusters at the Del Mar Seep with their roots penetrating carbonate rocks (Fig. 1G). We hypothesize that both the absence of mytilids and the scarcity of vestimentiferans are related to the oxygen environment, as they are also absent from other Pacific seeps occurring in the OMZ (Levin *et al.* 2010). The presence of these long-lived ecosystem engineers, however scarce, indicates persistence over decades or longer (Cordes *et al.* 2005), and the Del Mar Seep could play a role in regional connectivity patterns.

Community structure of macrofauna

As we hypothesized (H_2), sediments surrounding the Del Mar Seep exhibited an increase in macrofaunal density closer to the seep center. We found higher densities of polychaetes 32 m from the seep compared with 108 m away, and higher densities of mollusks 32 and 108 m

from the seep than 173 m away (Fig. 2). While proximity to the seep seemed to be associated with increases in the abundance of several macrofaunal groups, it did not contribute to a reduction in abundance of any taxa. These results support a role for the Del Mar Seep in providing trophic subsidies to the surrounding margin ecosystem. The sediments at the center of the seep (*e.g.* D_{amph} and E_{mat}) were species-poor and were likely physiologically stressful to all but seep endemics, but at tens to hundreds of meters away from the seep, macrofauna benefited from *in-situ* chemosynthetic production while avoiding high levels of hydrogen sulfide. Although diversity metrics and species richness were higher for all off-seep sediments than seep microhabitats, the overall effect of the seep was still to increase overall diversity (H_3). Much of this effect was likely due to faunal assemblages linked to particular microhabitats (Fig. S1).

We compared macrofaunal composition and diversity in sediments from the Del Mar Methane Seep with sediment macrofaunal communities from cold seeps across several regions and ocean basins (meta-analysis in Bernardino *et al.* 2012). Their study assessed sediment core data from different microhabitats, including background sediments. Our pooled data for the multicorer locations exhibited rarefaction diversity ($ES_{100} = 26$) nearly as high as for any of the seep sediment microhabitats examined in Bernardino *et al.* (2012). The macrofaunal community in background sediments from the Del Mar Seep cluster with those from northern California (Eel River) and Oregon (Hydrate Ridge) at the 65% similarity level, and they cluster with the active microhabitats (clam beds, bacterial mats) from those same seeps at the 55% similarity level. San Clemente seep background sediments, by contrast, are only 45% similar to the Del Mar Seep background sediments. Despite the geographic proximity between the San Clemente and Del Mar Seeps, depth and oxygen gradients have even stronger influences on these margin communities (Levin *et al.* 2010). Whereas the Del Mar Seep has bottom water oxygen of 0.4 ml·l^{-1} and is near the lower edge of the OMZ, San Clemente has a depth of 1800 m, much below the OMZ, and is relatively well oxygenated (Bernardino & Smith 2010). This is important for considering biodiversity patterns, as methane seeps along the same margin at multiple depths are likely to have greater beta diversity and potentially different types of ecosystem functions than multiple seeps along a single depth contour.

Chemosynthetic contribution to macrofaunal nutrition

We observed isotopically light carbon signatures in sediments over 100 m from any visible sign of chemosynthetic activity. While thick bacterial mats were not observed this

Table 3. Stable isotope signatures of macrofauna from all Del Mar Methane Seep microhabitats. Mean and SD of δ^{13}C and δ^{15}N per taxon, minimum (min.), and maximum (max.) percentage of methane-derived carbon (MDC), and total individuals (n). Note: Table S2 contains similar data except that macrofauna collected with multicorer in sediments away from the seep are included.

| taxonomic group/species | δ^{13}C | | δ^{15}N | | MDC percentage (%) | | |
	mean	SD	mean	SD	min.	max.	n
Annelida	−34.5	10.0	5.0	5.1	17	35	124
Ampharetidae	−34.6	5.5	4.1	3.9	9	35	19
Capitellidae	−24.5		9.2		0	9	1
Cirratulidae	−31.7	8.1	7.6	3.2	9	27	6
Dorvilleidae	−34.6	8.5	−0.5	4.2	15	35	19
Dorvillea sp.	−40.7	10.8	−2.2	3.6	33	51	6
Ophryotrocha sp.	−32.4	5.4	−0.4	3.6	6	29	9
Lacydoniidae	−24.8		14.2		0	9	1
Lumbrineridae	−28.4	6.6	9.2	4.1	4	19	4
Maldanidae	−37.5	12.7	7.5	3.2	24	43	2
Nephtyidae	−34.2		9.0		1	34	1
Nereidae	−44.7	7.5	2.5	4.1	41	62	16
Oligochaeta	−47.5	12.6	4.1	2.5	57	69	5
Orbiniidae	−32.6		10.5		0	30	1
Paraonidae	−23.7	2.0	10.5	1.6	0	7	6
Phyllodocidae	−21.7		12.0		0	1	1
Polynoidae	−29.6	3.9	8.6	3.7	1	22	8
Siboglinidae	−16.1	1.0	1.2	2.8	0	0	4
Escarpia spicata	−15.1		−3.0		0	0	1
Lamellibrachia barhami	−16.4	1.0	2.6	0.3	0	0	3
Siboglinum veleronis[a]	−31.9	4.0	6.8	5.2	5	29	14[a]
Sphaerodoridae	−29.1	0.4	10.6	3.8	0	21	2
Spionidae	−38.8	11.1	6.6	3.7	28	46	5
Syllidae	−29.6	7.1	8.7	4.5	5	22	9
Terebellidae	−40.0	6.8	4.4	3.9	26	49	11
Trichobranchidae	−50.6		−1.0		63	77	1
Chelicerata	−31.5	4.8	10.7	1.7	3	27	9
Cnidaria	−25.0	2.5	10.5	3.9	0	10	5
Anthozoa	−21.0		16.8		0	0	1
Hydrozoa	−26.0	1.2	9.0	2.0	0	13	4
Crustacea	−29.6	6.8	7.7	4.0	3	22	20
Amphipoda	−31.8	6.2	6.7	3.7	4	28	15
Decapoda	−25.7		7.7		0	12	1
Euphausiida	−20.5	1.6	10.5	0.2	0	1	2
Tanaidacea	−24.6	5.4	12.7	5.7	0	9	2
Ophiuroida	−23.8	2.8	10.0	1.7	0	7	9
Mollusca	−39.5	9.8	1.8	4.0	28	48	52
Aplacophora	−30.6	2.7	0.6	4.2	0	25	3
Bivalvia	−28.1	7.3	4.2	2.8	3	19	5
Protobranchia	−22.8	4.6	5.0	2.8	0	6	3
Vesicomyidae	−35.5	5.4	1.1	5.0	8	39	2
Gastropoda	−41.3	9.1	1.7	4.1	32	52	45
Astyris permodesta	−32.3		8.5		0	29	1
Cataegis sp.	−42.2		2.3		31	55	1
Hyalogyrina sp.	−53.5	7.9	2.4	4.3	74	84	3
Paralepetopsis sp.	−27.2	2.0	5.8	4.7	0	16	7
Provanna laevis	−41.4	7.4	1.5	3.4	29	53	15
Provanna lomana	−37.9	5.3	1.4	0.8	16	44	3
Pyropelta sp.	−46.4	4.7	−0.7	3.4	47	66	15
Nematoda	−31.1		−0.5		0	26	1
Nemertea	−26.5	3.9	10.4	3.5	0	14	8
Porifera	−35.8	11.1	8.8	3.3	21	38	7

Table 3. Continued

taxonomic group/species	δ13C		δ15N		MDC percentage (%)		
	mean	SD	mean	SD	min.	max.	n
Asbestopluma rickettsii	−27.2	3.5	6.9	2.9	0	16	4
Sponge, encrusting	−47.2	3.5	11.3	1.8	50	68	3
Sipuncula	−26.9		5.5		0	15	1
Protozoa	−28.1	6.1	5.1	5.4	2	18	9
Bathysiphon filiformis	−23.4	2.6	5.4	1.4	0	6	2
Arborescent foraminifera	−23.5	1.5	8.6	6.2	0	6	3
Folliculinid ciliates	−33.9	3.6	2.4	5.3	5	33	4
Filamentous bacteria	−29.6	5.4	2.4	3.8	3	22	14
Bacteria on carbonates	−32.4	5.3	1.2	2.4	6	29	8
Bacteria on sediments	−27.3	1.7	3.7	5.7	0	16	4

[a]Macrofauna from sediments away from the seep center and periphery are not included except for *Siboglinum veleronis* for comparison with other chemosynthetic taxa.

far from the seep center, we did find many chemosynthetic microbes within cores at B_{108} and C_{32}, often concentrated at the interface between aerobic and anaerobic sediments (5–7 cm deep). The ability of *Thioploca* and other sulfur bacteria to move vertically within their sheaths allows them to oxidize sulfide even when it is removed from their electron acceptors, thus allowing chemosynthetic production to occur despite oxygen in bottom waters (Fossing *et al.* 1995). Smaller taxa such as nematodes and oligochaetes may behave similarly, taking advantage of the microgradients in oxygen, sulfide, and nitrate in sediments (Levin 2005).

The average $\delta^{13}C$ for the macrofaunal community at location B_{108} was −22.3‰ compared with −20.1‰ at A_{173}. This modest difference in carbon signatures suggests that *in-situ* chemosynthetic production is being exported into sediments adjacent to the seep, which could explain the increase in macrofaunal densities nearer the seep. Individual macrofauna at A_{173} generally had stable isotope values reflecting photosynthetic production ($\delta^{13}C$ = −16 to −23‰); with the possible exceptions of bacterial filaments (−24.5‰), a dorvilleid (−24.7‰), and an agglutinated foraminiferan (−25.6‰) ($\delta^{13}C$ of sediment organic carbon was −21.1‰). Given our $\delta^{13}C$ signatures for potential end members ($\delta^{13}C_{POC}$ = −21.2‰; $\delta^{13}C_{CH4}$ = −59.9‰), the community at B_{108} could be receiving 0–2.9% of its carbon *via* methanotrophy, and its species composition reflected the greater influence of chemosynthetic production relative to A_{173}.

Certain taxa at B_{108} had $\delta^{13}C$ signatures clearly suggesting chemosynthetic sources of carbon. White bacterial filaments from sediments ($\delta^{13}C$ = −25.3‰ to −32.3‰) and symbiont-bearing species such as *Siboglinum veleronis* (−22.7‰ to −39.3‰) and a vesicomyid clam (−36.0‰) were able to access sulfide, despite living at a site (B_{108})

that might ordinarily be considered 'background sediments', highlighting the interactions between OMZ and seep-adapted faunas that are likely thiotrophic (Levin *et al.* 2010). Some chemosynthetic fauna typically observed in dense aggregations at seeps may be capable of living at many non-seep sites throughout the OMZ, as long as the sulfide–oxygen interface is shallow enough. Frenulates have been observed at other stations in the San Diego Trough (1000–1200 m, below the OMZ; Hartman 1961; C. A. Frieder, unpublished data), and we recovered a solemyid bivalve (*Acharax* sp.), which harbors sulfide oxidizers, from other stations within the OMZ. As hotspots of chemosynthetic productivity, both symbiont-bearing and heterotrophic fauna at methane seeps may represent source populations whose larvae enhance metapopulation connectivity regionally for a broader range of margin ecosystems.

Methane-derived carbon is clearly being incorporated into the macrofaunal food web in the areas of the Del Mar Seep that are most active – particularly carbonate rocks covered in microbial mats (H_4). Sulfide oxidation using the Rubisco I pathway often leads to $\delta^{13}C$ signatures between −27‰ and −37‰ for filamentous bacteria (Levin & Michener 2002; Zhang *et al.* 2005) and symbiont-bearing fauna (Conway *et al.* 1994), but approximately half the gastropods and one-third of the polychaetes sampled had $\delta^{13}C$ signatures between −40‰ and −60‰ (Fig. 5A). These isotopic signatures indicate that seep macrofauna incorporate MDC into their tissues. Microbes that perform AOM are often considered a benthic methane filter that reduces methane entering the water column (Sommer *et al.* 2006). Results from the Del Mar seep and other sites (Thurber *et al.* 2010; Rodrigues *et al.* 2013) suggest that seep macrofauna could represent another important component of this biological filter that sequesters methane carbon.
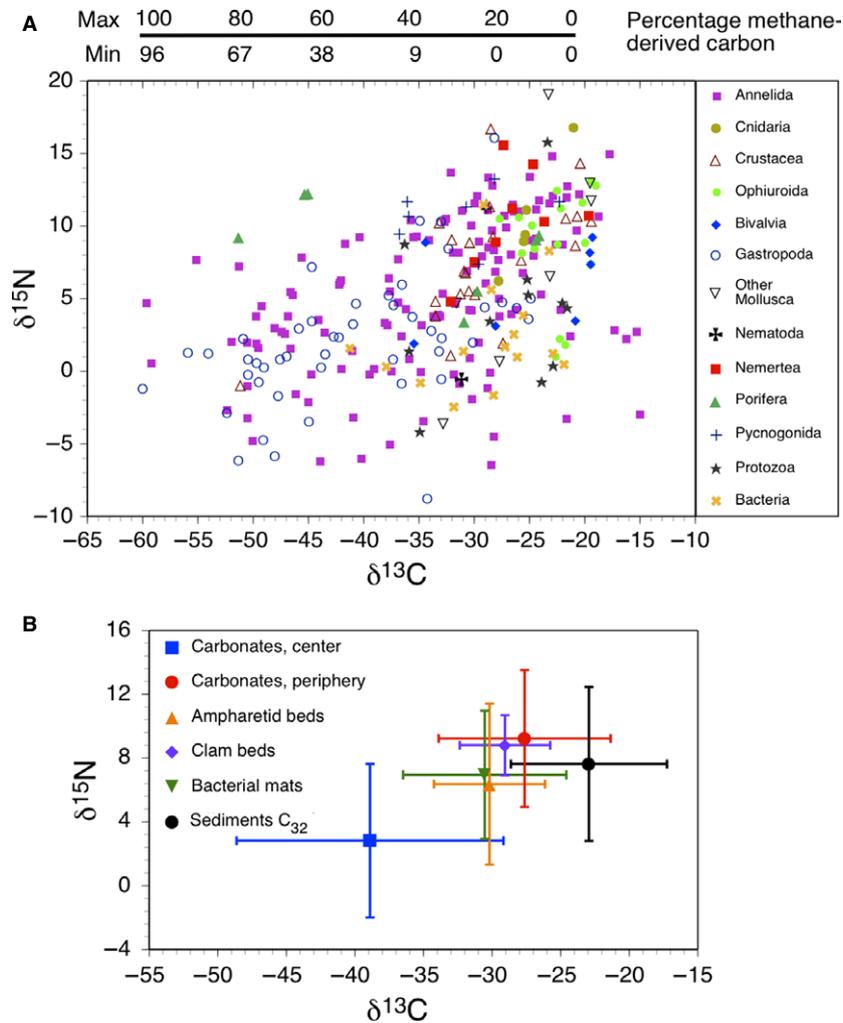
Fig. 5. (A): Stable isotope signatures of macrofauna, protists, and bacteria at the Del Mar Seep, including samples from all microhabitats. Minimum (Min) and maximum (Max) estimates of methane-derived carbon (MDC) are shown above the x-axis, where $\delta^{13}CH_4$ and $\delta^{13}C_{POC}$ are the end points for the maximum MDC, and $\delta^{13}CH_4$ and $\delta^{13}C_{SOB}$ are the end points for the minimum MDC; (B): stable isotope data of macrofauna in (A) are averaged for different microhabitats. 'Carbonates, center' are Rocks 1–3, while 'Carbonates, periphery' are Rocks 4–6. For sediments away from the seep, only C_{32} is shown because samples from A_{173} and B_{108} were not properly analysed for $\delta^{15}N$. Mean $\delta^{13}C$ of macrofauna at A_{173} (−20.1 ± 2.5) is greater than that at B_{108} (−22.2 ± 5.1) (statistics in text), but neither are significantly different from C_{32}.

Enhanced fish densities near the Del Mar Methane Seep

In addition to macrofauna, demersal fish and invertebrates were concentrated at the seep relative to nearby sedimented habitats (H_5). Densities of the longspine thornyhead, Pacific Dover sole and lithodid crabs, species often targeted by bottom fisheries, increased in the center and periphery of the Del Mar Seep relative to off-seep transects. In the case of *Sebastolobus altivelis*, densities in seep habitats were double those away from the seep (Fig. 6). The three-dimensionality of carbonate may offer a protective habitat, but thornyhead were about four times less numerous at a non-seep reference site 1 km away that also contained carbonates. Some aspect of a seep's chemical environment might play a role in enhancing or aggregating *S. altivelis*. This species is carnivorous on ophiuroids and other small benthic invertebrates (COSEWIC 2007), so the seep contains an abundance of potential prey items. Thornyheads are OMZ specialists

with low metabolic needs, and at 1000 m, biological maintenance may require a meal of just 5% of an individual's body mass every 150 days (Vetter & Lynn 1997). Thus, a relatively small, productive habitat such as the Del Mar Seep could likely support a high density of *S. altivelis*, and perhaps lead to enhanced growth rates compared with food-poor habitats. Alternatively, the chemical environment of the seep could benefit *S. altivelis* if it provides a refuge from predation (*e.g.* bearded goby in the Namibian OMZ, Salvanes *et al.* 2011) or acts to reduce parasite loads, as has been observed for other extremophile fish (Tobler *et al.* 2007).

Whether this represents aggregation around complex sea-floor habitat or trophic enhancement of a population, the results from this localized area suggest a possible link between methane seep habitats and rockfish. Associations between methane seeps and fisheries have been observed previously in Chile (Sellanes *et al.* 2008) and New Zealand (Bowden *et al.* 2013). Repeating ROV surveys at other
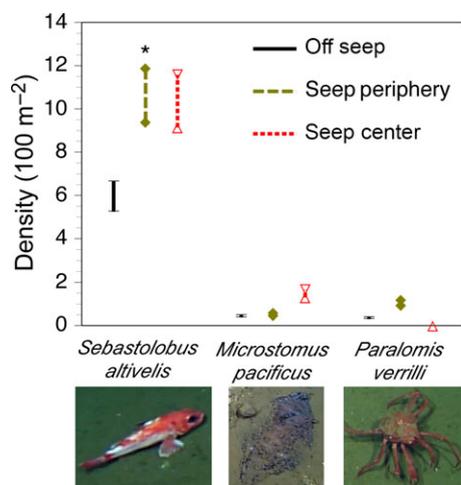
Fig. 6. Densities of groundfish and crabs observed in different habitat zones of the Del Mar Seep: Seep center (121–153 m² surveyed), seep periphery (337–426 m² surveyed), and off seep (1038–1315 m² surveyed). For each species, a maximum and minimum density per habitat zone, represented by connected points, were calculated based on uncertainty in the transect (3–3.8 m). *Represents non-randomly distributed individuals with respect to proportions of habitat zones (P < 0.05). Photo credits: MBARI.

seeps could help determine whether this interaction is site-specific or a regional pattern, but typical *S. altivelis* depth distributions (600–1700 m; Jacobson & Vetter 1996) potentially overlap with many seeps. Methane seeps are now known from several sites in the Southern California Bight (Torres *et al.* 2002; Paull *et al.* 2008; Bernardino & Smith 2010; present study), and can be regionally abundant in other Pacific locales such as Monterey Bay (Paull *et al.* 2005), Northern California (Levin & Michener 2002), and Costa Rica (Mau *et al.* 2006). The possibility that methane seeps could influence fish productivity is intriguing, as both thornyhead and Dover sole are important components of trawl fisheries (Stephens & Taylor 2013). Between 2003 and 2012, *Sebastolobus* spp. accounted for 3.5% of United States groundfish landings (US$7.3 million) and *Microstomus pacificus* accounted for 11.3% of landings (US$12.3 million) (Pacific Fishery Management Council 2014).

Conclusions

The continental margins are exposed to ever-increasing human activity, be it industrial (oil drilling, gas and minerals exploration, trawling), commercial (shipping traffic, cable laying) or recreational (fishing, whale-watching), and it is unclear how biodiversity and other ecosystem functions will respond (Levin & Sibuet 2012). In addition, the effects of climate change, specifically

impacting margins through deoxygenation, pH reduction, and altered productivity patterns, are expected to increase through the 21st century, potentially limiting the level of ecosystem services that the ocean provides to humans (Mora *et al.* 2013). Clearly methane seeps are involved in a host of ecosystem functions, some of which might be identified as ecosystem services if quantified and appropriately valued (*e.g.* fishery production or methanic carbon sequestration). This study highlights an important gap in continental margin research: namely, the lack of adequate measures or even descriptions of the ecosystem services methane seeps and other deep-sea chemosynthetic ecosystems provide (Thurber *et al.* 2014). Given the seeming ubiquity of cold seeps along global margins and the rapid discovery of new sites (Levin *et al.* 2012; Brothers *et al.* 2013), ecosystem services of methane seeps might be significant at a regional scale. Future research at methane seeps that quantifies trophic subsidies to other margin habitats, documents possible habitat relationships with fishery species, clearly defines links between diversity and ecosystem function, or explores the role of seeps as potential sources of larvae to surrounding habitats could serve as first steps in relating methane seep ecosystem functions to continental margin ecosystem services.

Acknowledgements

References

Armstrong C.W., Foley N.S., Tinch R., van den Hove S. (2012) Services from the deep: steps towards valuation of deep sea goods and services. *Ecosystem Services*, **2**, 2–13.

Barry J.P., Kochevar R.E. (1998) A tale of two clams: differing chemosynthetic life styles among vesicomyids in Monterey Bay cold seeps. *Cahiers de Biologie Marine*, **39**, 329–331.

Barry J.P., Greene H.G., Orange D.L., Baxter C.H., Robison B.H., Kochevar R.E., Nybakken J.W., Reed D.L., McHugh C.M. (1996) Biologic and geologic characteristics of cold seeps in Monterey Bay, California. *Deep-Sea Research Part I: Oceanographic Research Papers*, **43**, 1739–1762.

Barry J.P., Kochevar R.E., Baxter C.H. (1997) The influence of pore-water chemistry and physiology on the distribution of vesicomyid clams at cold seeps in Monterey Bay: implications for patterns of chemosynthetic community organization. *Limnology and Oceanography*, **42**, 318–328.

Bernardino A.F., Smith C.R. (2010) Community structure of infaunal macrobenthos around vestimentiferan thickets at the San Clemente cold seep, NE Pacific. *Marine Ecology*, **31**, 608–621.

Bernardino A.F., Levin L.A., Thurber A.R., Smith C.R. (2012) Comparative composition, diversity and trophic ecology of sediment macrofauna at vents, seeps and organic falls. *PLoS One*, **7**, e33515.

Boetius A., Wenzhöfer F. (2013) Seafloor oxygen consumption fuelled by methane from cold seeps. *Nature Geoscience*, **6**, 725–734.

Bowden D.A., Rowden A.A., Thurber A.R., Baco A.R., Levin L.A., Smith C.R. (2013) Cold seep epifaunal communities on the Hikurangi Margin, New Zealand: composition, succession, and vulnerability to human activities. *PLoS One*, **8**, e76869.

Brothers L.L., Van Dover C.L., German C.R., Kaiser C.L., Yoerger D.R., Ruppel C.D., Lobecker E., Skarke A.D., Wagner J.K.S. (2013) Evidence for extensive methane venting on the southeastern U.S. Atlantic margin. *Geology*, **41**, 807–810.

Cline J.D. (1969) Spectrophotometric determination of hydrogen sulfide in natural waters. *Limnology & Oceanography*, **14**, 454–458.

Conway N., Kennicutt M. II, Van Dover C. (1994) Stable isotopes in the study of marine chemosynthetic-based ecosystems. In: Lajtha K., Michener R. (Eds), *Stable Isotopes in Ecology and Environmental Sciences: Methods in Ecology*. Blackwell Scientific, Oxford: 158–186.

Cordes E.E., Hourdez S., Predmore B.L., Redding M.L., Fisher C.R. (2005) Succession of hydrocarbon seep communities associated with the long-lived foundation species *Lamellibrachia luymesi*. *Marine Ecology Progress Series*, **305**, 17–29.

Cordes E.E., Cunha M.R., Galéron J., Mora C., Olu-Le Roy K., Sibuet M., Van Gaever S., Vanreusel A., Levin L.A. (2010) The influence of geological, geochemical, and biogenic

habitat heterogeneity on seep biodiversity. *Marine Ecology*, **31**, 51–65.

COSEWIC (2007) *COSEWIC Assessment and Status Report on the Longspine Thornyhead* Sebastolobus altivelis *in Canada*. Committee on the Status of Endangered Wildlife in Canada, Ottowa: 27.

Danovaro R., Gambi C., Dell'Anno A., Corinaldesi C., Fraschetti S., Vanreusel A., Vincx M., Gooday A.J. (2008) Exponential decline of deep-sea ecosystem functioning linked to benthic biodiversity loss. *Current Biology*, **18**, 1–8.

De Leo F.C., Smith C.R., Rowden A.A., Bowden D.A., Clark M.R. (2010) Submarine canyons: hotspots of benthic biomass and productivity in the deep sea. *Proceedings of the Royal Society B*, **277**, 2783–2792.

Decker C., Morineaux M., Van Gaever S., Caprais J.-C., Lichtschlag A., Gauthier O., Andersen A.C., Olu K. (2012) Habitat heterogeneity influences cold-seep macrofaunal communities within and among seeps along the Norwegian margin. Part 1: macrofaunal community structure. *Marine Ecology*, **33**, 205–230.

Dekas A.E., Poretsky R.S., Orphan V.J. (2009) Deep-sea archaea fix and share nitrogen in methane-consuming microbial consortia. *Science*, **326**, 422–426.

Drazen J.C., Goffredi S.K., Schlining B., Stakes D.S. (2003) Aggregations of egg-brooding deep-sea fish and cephalopods on the Gorda Escarpment: A reproductive hot spot. *Biological Bulletin*, **205**, 1–7.

Fossing H., Gallardo V.A., Jørgensen B.B., Hüttel M., Nielsen L.P., Schulz H., Canfield D.E., Forster S., Glud R.N., Gundersen J.K., Küver J., Ramsing N.B., Teske A., Thamdrup B., Ulloa O. (1995) Concentration and transport of nitrate by the mat-forming sulphur bacterium *Thioploca*. *Nature*, **374**, 713–715.

Fry B. (2006) *Stable Isotope Ecology*. Springer, New York: 308.

Fry B., Sherr E.B. (1984) δ^{13}C measurements as indicators of carbon flow in marine and freshwater ecosystems. *Contributions in Marine Science*, **27**, 13–47.

Gooday A., Levin L.A., Thomas C., Hecker B. (1992) The distribution and ecology of *Bathysiphon filiformis* Sars and *B. major* de Folin (Protista, Foraminiferida) on the continental slope off North Carolina. *The Journal of Foraminiferal Research*, **22**, 129–146.

Green-Saxena A., Feyzullayev A., Hubert C.R.J., Kallmeyer J., Krueger M., Sauer P., Schulz H.M., Orphan V.J. (2012) Active sulfur cycling by diverse mesophilic and thermophilic microorganisms in terrestrial mud volcanoes of Azerbaijan. *Environmental Microbiology*, **14**, 3271–3286.

Hartman O. (1961) New pogonophora from the Eastern Pacific Ocean. *Pacific Science*, **15**, 542–546.

Hilário A., Cunha M.R. (2008) On some frenulate species (Annelida: Polychaeta: Siboglinidae) from mud volcanoes in the Gulf of Cadiz (NE Atlantic). *Scientia Marina*, **72**, 361–371.

Hilário A., Capa M., Dahlgren T.G., Halanych K.M., Little C.T.S., Thornhill D.J., Verna C., Glover A.G. (2011) New

perspectives on the ecology and evolution of siboglinid tubeworms. *PLoS One*, **6**, e16309.

Hinrichs K.U., Boetius A. (2002) The anaerobic oxidation of methane: new insights in microbial ecology and biogeochemistry. In: Wefer G., Billett D., Hebbeln D., Jørgensen B.B., Schlüter M., Van Weering T. (Eds), *Ocean Margin Systems*. Springer-Verlag, Berlin: 457–477.

Jacobson L.D., Vetter R.D. (1996) Bathymetric demography and niche separation of thornyhead rockfish: *Sebastolobus alascanus* and *Sebastolobus altivelis*. *Canadian Journal of Fisheries and Aquatic Sciences*, **53**, 600–609.

Kulm L.D., Suess E., Moore J.C., Carson B., Lewis B.T., Ritger S.D., Kadko D.C., Thornburg T.M., Embley R.W., Rugh W.D., Massoth G.J., Langseth M.G., Cochrane G.R., Scamman R.L. (1986) Oregon subduction zone: venting, fauna, and carbonates. *Science*, **231**, 561–566.

Levin L.A. (2005) Ecology of cold seep sediments: interactions of fauna with flow, chemistry and microbes. *Oceanography and Marine Biology: An Annual Review*, **43**, 1–46.

Levin L.A., Dayton P.K. (2009) Ecological theory and continental margins: where shallow meets deep. *Trends in Ecology & Evolution*, **24**, 606–617.

Levin L.A., Mendoza G.F. (2007) Community structure and nutrition of deep methane-seep macrobenthos from the North Pacific (Aleutian) Margin and the Gulf of Mexico (Florida Escarpment). *Marine Ecology*, **28**, 131–151.

Levin L.A., Michener R.H. (2002) Isotopic evidence for chemosynthesis-based nutrition of macrobenthos: the lightness of being at Pacific methane seeps. *Limnology and Oceanography*, **47**, 1336–1345.

Levin L.A., Sibuet M. (2012) Understanding continental margin biodiversity: a new imperative. *Annual Review of Marine Science*, **4**, 79–112.

Levin L.A., Ziebis W., Mendoza G.F., Growney V.A., Tryon M.D., Brown K.M., Mahn C., Gieskes J.M., Rathburn A.E. (2003) Spatial heterogeneity of macrofauna at northern California methane seeps: influence of sulfide concentration and fluid flow. *Marine Ecology Progress Series*, **265**, 123–139.

Levin L.A., Mendoza G.F., Gonzalez J.P., Thurber A.R., Cordes E.E. (2010) Diversity of bathyal macrofauna on the northeastern Pacific margin: the influence of methane seeps and oxygen minimum zones. *Marine Ecology*, **31**, 94–110.

Levin L.A., Orphan V.J., Rouse G.W., Rathburn A.E., Ussler W., Cook G.S., Goffredi S.K., Perez E.M., Waren A., Grupe B.M., Chadwick G., Strickrott B. (2012) A hydrothermal seep on the Costa Rica margin: middle ground in a continuum of reducing ecosystems. *Proceedings of the Royal Society B*, **279**, 2580–2588.

Levin L.A., Ziebis W., Mendoza G., Bertics V.J., Washington T., Gonzalez J., Thurber A.R., Ebbe B., Lee R.W. (2013) Ecological release and niche partitioning under stress: lessons from dorvilleid polychaetes in sulfidic sediments at methane seeps. *Deep-Sea Research Part II: Topical Studies in Oceanography*, **92**, 214–233.

Lundsten L., Reiswig H.M., Austin W.C. (2014) Four new species of Cladorhizidae (Porifera, Demospongiae, Poecilosclerida) from the Northeast Pacific. *Zootaxa*, **3786**, 101–123.

Maloney J.M. (2013) *Fault segments and step-overs: implications for geohazards and biohabitats*. Ph.D. Dissertation University of California, San Diego, La Jolla, California: 210.

Mau S., Sahling H., Rehder G., Suess E., Linke P., Soeding E. (2006) Estimates of methane output from mud extrusions at the erosive convergent margin off Costa Rica. *Marine Geology*, **225**, 129–144.

Mora C., Wei C.-L., Rollo A., Amaro T., Baco A.R., Billett D., Bopp L., Chen Q., Collier M., Danovaro R., Gooday A.J., Grupe B.M., Halloran P.R., Ingels J., Jones D.O.B., Levin L.A., Nakano H., Norling K., Ramirez-Llodra E., Rex M., Ruhl H.A., Smith C.R., Sweetman A.K., Thurber A.R., Tjiputra J.F., Usseglio P., Watling L., Wu T., Yasuhara M. (2013) Biotic and human vulnerability to projected changes in ocean biogeochemistry over the 21st century. *PLoS Biology*, **11**, e1001682.

Niemann H., Linke P., Knittel K., MacPherson E. (2013) Methane-carbon flow into the benthic food web at cold seeps – A case study from the Costa Rica subduction zone. *PLoS One*, **8**, e74894.

Pacific Fishery Management Council (2014) *Groundfish Harvest Specifications and Management Measures and Amendment 24: Draft Environmental Impact Statement*. Pacific Fisheries Management Council, Portland, OR: 502.

Paull C.K., Schlining B., Ussler W., Paduan J.B., Caress D., Greene H.G. (2005) Distribution of chemosynthetic biological communities in Monterey Bay, California. *Geology*, **33**, 85–88.

Paull C.K., Normark W.R., Ussler W., Caress D.W., Keaten R. (2008) Association among active seafloor deformation, mound formation, and gas hydrate growth and accumulation within the seafloor of the Santa Monica Basin, offshore California. *Marine Geology*, **250**, 258–275.

Reeburgh W.S. (2007) Oceanic methane biogeochemistry. *Chemical Reviews*, **107**, 486–513.

Ritger S., Carson B., Suess E. (1987) Methane-derived authigenic carbonates formed by subduction-induced pore-water expulsion along the Oregon/Washington margin. *Geological Society of America Bulletin*, **98**, 147.

Ritt B., Sarrazin J., Caprais J.-C., Noël P., Gauthier O., Pierre C., Henry P., Desbruyéres D. (2010) First insights into the structure and environmental setting of cold-seep communities in the Marmara Sea. *Deep-Sea Research Part I: Oceanographic Research Papers*, **57**, 1120–1136.

Rodrigues C.F., Hilário A., Cunha M.R. (2013) Chemosymbiotic species from the Gulf of Cadiz (NE Atlantic): distribution, life styles and nutritional patterns. *Biogeosciences*, **10**, 2569–2581.

Ryan H.F., Conrad J.E., Paull C.K., McGann M. (2012) Slip rate on the San Diego trough fault zone, inner California Borderland, and the 1986 Oceanside earthquake swarm

revisited. *Bulletin of the Seismological Society of America*, **102**, 2300–2312.

Sahling H., Rickert D., Lee R.W., Linke P., Suess E. (2002) Macrofaunal community structure and sulfide flux at gas hydrate deposits from the Cascadia convergent margin, NE Pacific. *Marine Ecology Progress Series*, **231**, 121–138.

Sahling H., Wallmann K., Dahlmann A., Schmaljohann R., Petersen S. (2005) The physicochemical habitat of *Sclerolinum* sp. at Hook Ridge hydrothermal vent, Bransfield Strait, Antarctica. *Limnology and Oceanography*, **50**, 598–606.

Salvanes A.G.V., Utne-Palm A.C., Currie B., Braithwaite V.A. (2011) Behavioural and physiological adaptations of the bearded goby, a key fish species of the extreme environment of the northern Benguela upwelling. *Marine Ecology Progress Series*, **425**, 193–202.

Sellanes J., Quiroga E., Neira C. (2008) Megafauna community structure and trophic relationships at the recently discovered Concepción Methane Seep Area, Chile, ∼36° S. *ICES Journal of Marine Science: Journal du Conseil*, **65**, 1102–1111.

Sellanes J., Pedraza M.J., Zapata Hernandez G. (2012) Las areas de filtracion de metano constituyen zonas de agregación del bacalao de profundidad (*Dissostichus eleginoides*) frente a Chile central. *Latin American Journal of Aquatic Research*, **40**, 980–991.

Sommer S., Pfannkuche O., Linke P., Luff R., Greinert J., Drews M., Gubsch S., Pieper M., Poser M., Viergutz T. (2006) Efficiency of the benthic filter: biological control of the emission of dissolved methane from sediments containing shallow gas hydrates at Hydrate Ridge. *Global Biogeochemical Cycles*, **20**, GB2019.

Stephens A., Taylor I.G. (2013) *Stock Assessment and Status of Longspine Thornyhead (*Sebastolobus altivelis*) off California, Oregon and Washington in 2013*. Pacific Fisheries Management Council, Seattle, Washington: 123.

Thurber A.R., Kröger K., Neira C., Wiklund H., Levin L.A. (2010) Stable isotope signatures and methane use by New Zealand cold seep benthos. *Marine Geology*, **272**, 260–269.

Thurber A.R., Levin L.A., Rowden A.A., Sommer S., Linke P., Kröger K. (2013) Microbes, macrofauna, and methane: a novel seep community fueled by aerobic methanotrophy. *Limnology and Oceanography*, **58**, 1640–1656.

Thurber A.R., Sweetman A.K., Narayanaswamy B.E., Jones D.O.B., Ingels J., Hansman R.L. (2014) Ecosystem function and services provided by the deep sea. *Biogeosciences*, **11**, 3941–3963.

Tobler M., Schlupp I., García de León F.J., Glaubrecht M., Plath M. (2007) Extreme habitats as refuge from parasite infections? Evidence from an extremophile fish. *Acta Oecologica*, **31**, 270–275.

Torres M.E., McManus J., Huh C. (2002) Fluid seepage along the San Clemente Fault scarp: basin-wide impact on barium cycling. *Earth and Planetary Science Letters*, **203**, 181–194.

Treude T. (2012) Biogeochemical reactions in marine sediments underlying anoxic water bodies. In: Altenbach A.V., Bernhard J.M., Seckbach J. (Eds), *Anoxia: Evidence for Eukaryotic Survival and Paleontological Strategies*. Springer, Dordrecht: 17–38.

Treude T., Kiel S., Linke P., Peckmann J., Goedert J.L. (2011) Elasmobranch egg capsules associated with modern and ancient cold seeps: a nursery for marine deep-water predators. *Marine Ecology Progress Series*, **437**, 175–181.

Vetter R.D., Lynn E.A. (1997) Bathymetric demography, enzyme activity patterns, and bioenergetics of deep-living scorpaenid fishes (genera *Sebastes* and *Sebastolobus*): Paradigms revisited. *Marine Ecology Progress Series*, **155**, 173–188.

Whiticar M.J. (1999) Carbon and hydrogen isotope systematics of bacterial formation and oxidation of methane. *Chemical Geology*, **161**, 291–314.

Zhang C.L., Huang Z., Cantu J., Pancost R.D., Brigmon R.L., Lyons T.W., Sassen R. (2005) Lipid biomarkers and carbon isotope signatures of a microbial (*Beggiatoa*) mat associated with gas hydrates in the Gulf of Mexico. *Applied and Environmental Microbiology*, **71**, 2106–2112.

Supporting Information

Additional Supporting Information may be found in the online version of this article:

Figure S1. Dendogram of the clustering relationships among sediment core and carbonate communities, performed on a Bray–Curtis resemblance matrix.

Table S1. Hydrographic and sediment physical and chemical parameters at Del Mar Methane Seep.

Table S2. SIMPER results for community analysis.

Table S3. Stable isotope signatures (mean and SD of $\delta^{13}C$ and $\delta^{15}N$) of macrofauna, protists, and bacteria by taxa, minimum and maximum methane-derived carbon (MDC), and total samples analyzed (Replicates).

Table S4. Sensitivity analysis testing the effect of a $\pm$ 10% change in the value for $\delta^{13}CH_4$ (the end member in the isotopic mixing model) on estimates of the range of methane-derived carbon (MDC) for common faunal groups.

Video S1. Video from ROV surveys over the seep center and seep periphery, highlighting extensive microbial mats, authigenic carbonates, methane bubbling, and megafauna.

Video S2. Closeup video of *Lamellibrachia barhami*, microbial mats, and carbonates.